Check for updates

Angewandte Chemie International Edition

Angewandte International Edition Chemie

How to cite: *Angew. Chem. Int. Ed.* **2026**, 65, e5110668
doi.org/10.1002/anie.5110668

RESEARCH ARTICLE

Kinetically Stereocontrolled *Gem*-Fluoro(chloro)-Olefination of Carbonyls by an Unprecedented Sulfoximine: Programmable Construction of Challenging Persubstituted Alkenyl Fluorides

Han Yu[1] | Gaoyang Ni[1] | Qingyuan Zhao[1] | Yanbo Peng[1] | Shiyu Pan[1] | Jing Zhang[1] | Quan Liu[2] | Tian-Yu Sun[3] | Jinbo Hu[4] | Qinghe Liu[1]

[1]State Key Laboratory of Natural Medicines, Department of Pharmaceutical Engineering, China Pharmaceutical University, Nanjing, P.R. China | [2]Shanghai PROXS Chemical Technology Co. Ltd, Shanghai, P.R. China | [3]Key Lab of Computational Chemistry and Drug Design, State Key Laboratory of Chemical Oncogenomics, School of Chemical Biology and Biotechnology, Shenzhen Key Laboratory of Chemical Genomics, Peking University Shenzhen Graduate School, Shenzhen, P.R. China | [4]State Key Laboratory of Fluorine and Nitrogen Chemistry and Advanced Materials, Center For Excellence in Molecular Synthesis, Shanghai Institute of Organic Chemistry, University of Chinese Academy of Sciences, Chinese Academy of Sciences, Shanghai, P.R. China

Correspondence: Jing Zhang (jingzhang@cpu.edu.cn) | Tian-Yu Sun (Tian-Yu_Sun@pku.edu.cn) | Jinbo Hu (jinbohu@sioc.ac.cn) | Qinghe Liu (qingheliu@cpu.edu.cn)

Received: 2 December 2025 | **Revised:** 24 January 2026 | **Accepted:** 11 February 2026

Keywords: gem-fluoro(chloro)olefination | nucleophilic | persubstituted alkenyl fluorides | stereoselective | sulfoximine

ABSTRACT

Persubstituted alkenyl fluorides represent pivotal motifs in drug discovery, agrochemical development, and biological science. The *(E)*-isomeric persubstituted alkenyl fluoride, widely recognized as a conformationally stable mimic of the amide bond, frequently exhibits significantly higher bioactivity than the *(Z)*-counterpart. Despite their potential, the synthesis of this scaffold remains challenging, due to the severe steric encumbrance. Herein, we reported a highly stereoselective carbonyl *gem*-fluoro(chloro)olefination with an unprecedented sulfoximine reagent, affording an array of *(Z)*-persubstituted gem-fluoro(chloro)alkenes. Subsequent cross-couplings enabled them rapidly into a wide array of challenging stereodefined *(E)*- or *(Z)*-alkenyl fluorides. The experimental and computational data demonstrated that the key mechanistic feature involved a predominant 1,5-attack pathway, which operated as the rate-determining step with kinetic stereocontrol and prevailed over both the 1,3- and 1,4-attack pathways. The synthetic utility was demonstrated through microfluid synthesis, late-stage modifications, and a streamlined stereoselective synthesis of factor Xa inhibitor and RXR regulator.

1 | Introduction

Fluorine-containing organic molecules are highly valuable, because introduction of fluorine into organic molecules often endows the higher metabolic stability, cell membrane permeability, and bioavailability than their nonfluorinated counterparts [1–9]. Tetrasubstituted alkenyl fluorides are a noteworthy subclass of these compounds, and the moiety has been recognized as a privileged motif and often presented in impact biological active compounds [7], such as factor D inhibitors [10], retinoid X receptor regulators [11], and Alzheimer's-targeting thymidyl-PNA monomers [12] (Figure 1a). Their unique advantages could be

Dedicated to the 90th anniversary of China Pharmaceutical University

© 2026 Wiley-VCH GmbH

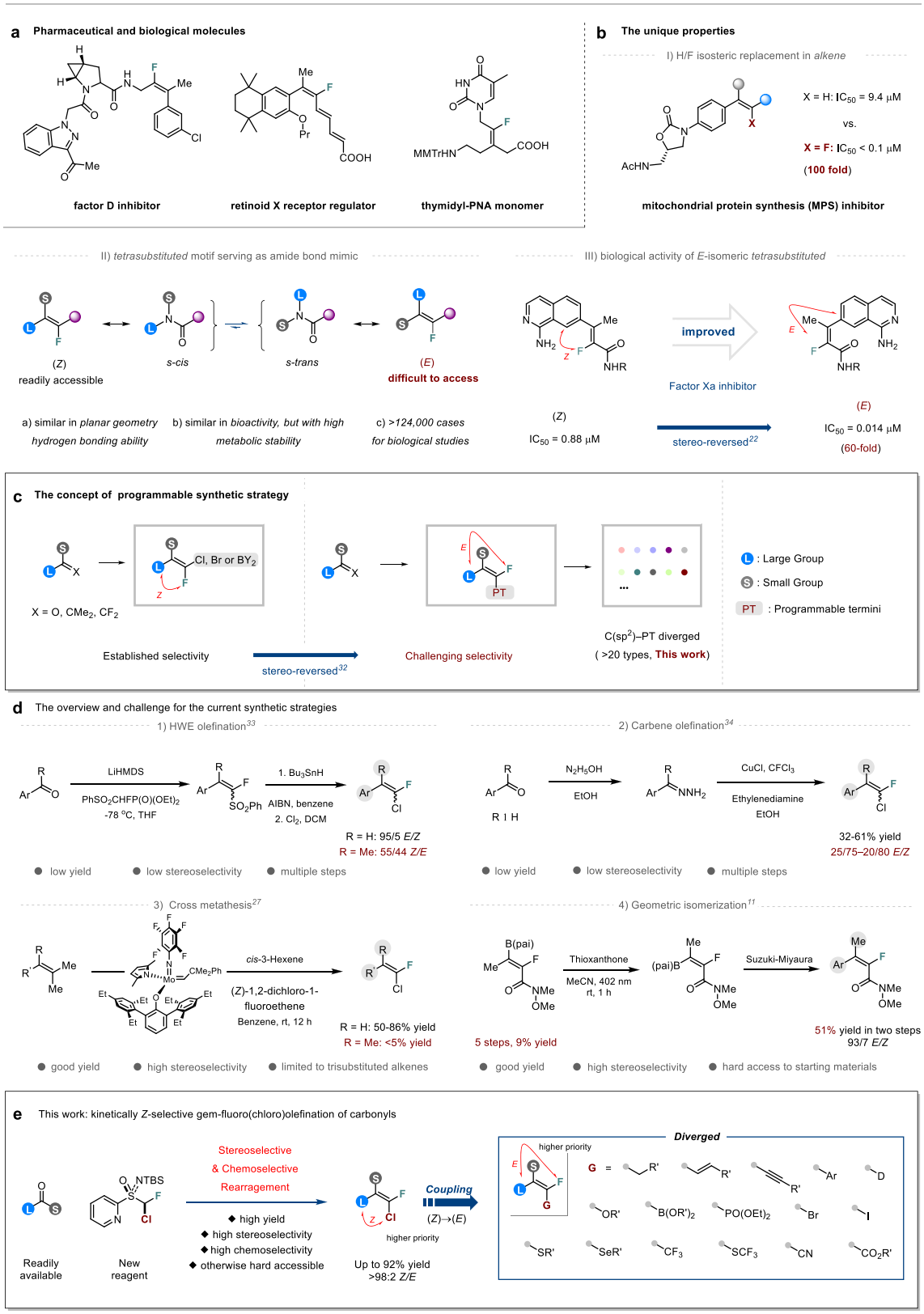


FIGURE 1 | The significance of (*E*)-persubstituted alkenyl fluorides, and the concept, state of the art and the hypothesized highly stereoselective *gem*-fluoro(chloro)-olefination of carbonyl compounds. (a) Examples of pharmaceutical and bioactive molecules with persubstituted alkenyl fluoride moieties. (b) The unique biological properties of persubstituted alkenyl fluoride moieties. (I) The H/F replacement can improve the bioactivities of compounds in alkenes; (II) alkenyl fluorides motif can mimic amide bond in peptides; (III) *E*-isomeric persubstituted alkenyl fluoride presents higher biological activity than its *Z*-analogue. (c) The concept of divergent synthesis based on synthetic programmable termini strategy. (d) The overview and challenge for the current synthetic strategies. (e) The first highly stereoselective *gem*-fluoro(chloro)olefination of carbonyls with an unprecedented sulfoximine reagent. CC, cross coupling; HWE, Horner–Wadsworth–Emmons; MPS, mitochondrial protein synthesis; pai, pinanediol.

15213773, 2026, 15, Downloaded from https://onlinelibrary.wiley.com/doi/10.1002/anie.511068 by Shanghai Institute Of Organic Chemistry, Wiley Online Library on [03/11/2026]. See the Terms and Conditions (https://onlinelibrary.wiley.com/terms-and-conditions) on Wiley Online Library for rules of use; OA articles are governed by the applicable Creative Commons License

attributed to the following: 1) Substituting a hydrogen atom with fluorine at a C═C bond often improved the parent molecule's physicochemical properties and biological activity by enhancement of physicochemical stability [2, 13, 14]. For example, the fluorine-modified mitochondrial protein synthesis (MPS) inhibitor exhibited over 100-fold higher activity than its nonfluorinated analogue (Figures 1b, I) [15, 16]. 2) An alkenyl fluoride fragment served as an effective amide bioisostere due to its ability to mimic the planar geometry of the amide, despite having a smaller dipole moment and a significantly lower hydrogen-bond accepting ability. [17–19]. Incorporating this motif into peptide or protein-based drugs can prevent enzymatic hydrolysis of amide by peptidases/proteases, thereby enhancing metabolic stability (Figures 1b, II) [20]. And 3) from a stereochemical perspective, (*Z*)-alkenyl fluorides mimicked the *s-cis* amide conformation, while (*E*)-analogues replicated the *s-trans* as thermodynamically-favored conformation [21]. This substitution restricts C═C bond rotation, yielding conformationally locked peptidomimetics and often exhibiting superior performance relative to (*Z*)-analogues. A canonical example is that the (*E*)-alkenyl fluoride-based factor Xa inhibitor demonstrated over 60-fold higher activity than its (*Z*)-counterpart (Figures 1b, III) [22]. Therefore, given the pharmacological importance, to develop a streamlined, stereocontrolled approach is highly attractive and critical for drug discovery and development [7, 23–28].

However, a superior route for the synthesis of this class of compounds is to introduce a programmable termini (i.e., an easily modifiable group), such as a halogen, at the fluorinated carbon terminus [29–31], which enables rapid diversification into structurally diverse alkenyl fluorides. Nevertheless, the strategies to date have been severely limited to (*Z*)-configured alkenyl fluorides (Figure 1c, left) [26–28], and there are substantial synthetic barriers to the *stereo-reversed* version [32] (Figure 1c, middle). Despite several methods for synthesis of (*E*)-persubstituted alkenyl fluorides with programmable termini have been reported, the challenges inherent can also be inferred from these findings. A Horner–Wadsworth–Emmons reaction followed by a two-step transformation provided persubstituted fluoro(chloro)alkenes, but it required three steps and achieved only 55:44 *Z*/*E* stereoselectivity (Figures 1d, I) [33]. Copper-carbene complex formation from hydrazone gave persubstituted alkenes with a fluoro-chloro terminus, but both the yields and stereoselectivities were low (Figures 1d, II) [34]. Molybdenum-catalyzed cross metathesis gave *gem*-fluoro(chloro)alkenes with excellent stereocontrol, but this approach was limited to tri-substituted homologs (Figures 1d, III) [27]. The desired stereoisomer of alkenyl fluorides with Weinreb amide terminus, could be obtained via geometric isomerization by energy transfer catalysis of thioxanthone, but the approach was limited by multiple steps and the low efficiency of the starting material preparation (Figures 1d, IV) [11]. Therefore, the highly stereoselective synthesis of (*E*)-persubstituted fluoroalkenes bearing a programmable terminus remains an unmet synthetic challenge.

Fluorinated sulfoximines have emerged as versatile reagents for the asymmetric synthesis of organofluorines, yet their use in monofluoroolefin construction remains underexplored [35–41]. Existing fluoro-olefination strategies are constrained by the presence of a hydrogen atom at the fluoro terminus, severely limiting their structural diversification [42]. Nevertheless, inspired by the steric discrimination capability of the sulfoximidoyl group, we hypothesized that a stereoselective Smiles rearrangement could be performed using a new reagent, *S*-fluorochloromethyl-*S*-pyridyl sulfoximine (Figure 1e, left). To the best of our knowledge, no stereoselective chloro-tagged olefination reaction between sulfoximine and carbonyls has been reported, because of the physical properties of chlorine atom and the observed preferential C—Cl bond cleavage [43, 44]. However, we expected that the strong electrophilic character of the pyridyl moiety introduced, would protect the C—Cl bond against premature bond cleavage. And the introduced silyl group could stabilize the neighboring nitrogen anion during the Smiles rearrangement.

Therefore, an efficient and stereocontrolled approach for synthesizing (*Z*)-persubstituted *gem*-fluoro(chloro)alkenes through a kinetically controlled *gem*-fluoro(chloro)olefination was developed in this work. It was worthy to note the developed *sulfoximine reagent* was the first example of sulfoximine reagent bearing mixed *gem*-halides [45–47]. This method employed readily available carbonyl compounds, enhancing its synthetic utility significantly [48, 49]. The subsequent cross couplings enabled rapid access to an assortment of (*E*)- or (*Z*)-persubstituted alkenyl fluorides, further improving its significance (Figure 1e, right). The utilization was demonstrated by microfluid synthesis, late-stage modification, and streamlined stereoselective synthesis of factor Xa inhibitor and RXR regulator. The experimental and computational data uncovered that the key mechanistic feature involved a predominant 1,5-attack pathway, which prevailed over both the 1,3- and 1,4-attack pathways and operated as the rate-determining by kinetic stereocontrol.

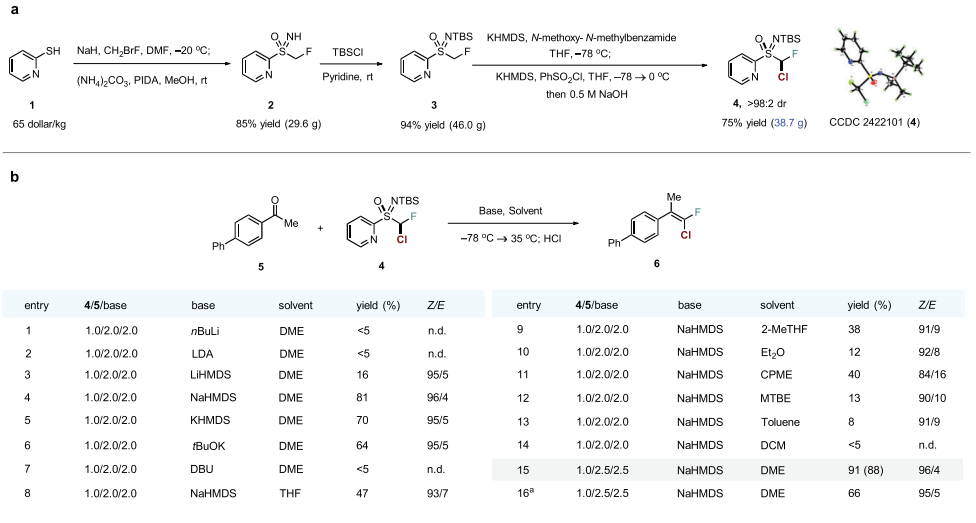
2 | Results and Discussion

2.1 | Initial Discovery of Stereoselective Nucleophilic Gem-Fluoro(chloro)-Olefination

We developed a method for the preparation of S-fluorochloromethyl-S-pyridyl sulfoximine (**4**). First, compound **2** was obtained in 85% yield from the cheap starting material of 2-mercaptopyridine, which was further transformed to compound 3 by reacting with TBSCl. Compound **3** underwent benzylation upon reaction with a Weinreb amide, followed by chlorination with a sulfonyl chloride. Finally, deprotection of the benzoyl group in sodium hydroxide solution afforded the target product **4** (Figure 2a). Scaling up the procedure afforded **4** on a scale of 38.7 g, and the relative configuration was unambiguously determined by X-ray crystallographic analysis [50]. Structural analysis revealed that the relative configuration of sulfur exerts a significant steric influence on the relative configuration of the adjacent carbon.

With reagent **4** in hand, we investigated the stereoselective synthesis of persubstituted fluoro(chloro)alkenes via an α-fluorinated carbanion strategy. Acetophenone (**5**) was chosen as a model substrate; the results are summarized in Figure 2b. Typically, a base was added to the mixture of **4** and **5**, and the ratio of **4**:**5**:base was 1.0:2.0:2.0. When *n*BuLi or LDA was used as the base, no fluoro(chloro)alkene was detected on ^{19}F NMR spectroscopy (Figure 2b, entries 1 and 2). When the base was changed to lithium hexamethyldisilazide (LiHMDS), a yield of

15213773, 2026, 15, Downloaded from https://onlinelibrary.wiley.com/doi/10.1002/anie.511068 by Shanghai Institute Of Organic Chemistry, Wiley Online Library on [03/11/2026]. See the Terms and Conditions (https://onlinelibrary.wiley.com/terms-and-conditions) on Wiley Online Library for rules of use; OA articles are governed by the applicable Creative Commons License



entry	4/5/base	base	solvent	yield (%)	Z/E	entry	4/5/base	base	solvent	yield (%)	Z/E
1	1.0/2.0/2.0	*n*BuLi	DME	<5	n.d.	9	1.0/2.0/2.0	NaHMDS	2-MeTHF	38	91/9
2	1.0/2.0/2.0	LDA	DME	<5	n.d.	10	1.0/2.0/2.0	NaHMDS	Et_2O	12	92/8
3	1.0/2.0/2.0	LiHMDS	DME	16	95/5	11	1.0/2.0/2.0	NaHMDS	CPME	40	84/16
4	1.0/2.0/2.0	NaHMDS	DME	81	96/4	12	1.0/2.0/2.0	NaHMDS	MTBE	13	90/10
5	1.0/2.0/2.0	KHMDS	DME	70	95/5	13	1.0/2.0/2.0	NaHMDS	Toluene	8	91/9
6	1.0/2.0/2.0	*t*BuOK	DME	64	95/5	14	1.0/2.0/2.0	NaHMDS	DCM	<5	n.d.
7	1.0/2.0/2.0	DBU	DME	<5	n.d.	15	1.0/2.5/2.5	NaHMDS	DME	91 (88)	96/4
8	1.0/2.0/2.0	NaHMDS	THF	47	93/7	16[a]	1.0/2.5/2.5	NaHMDS	DME	66	95/5

FIGURE 2 | Synthesis of *gem*-fluoro(chloro)methyl sulfoximine and the reaction discovery. (a) The synthetic route of *gem*-fluoro(chloro)methyl pyridyl sulfoximine from the commercially available starting materials. (b) The investigation of the reaction conditions. General reaction conditions: Base was added slowly to the mixture of **4** (0.2 mmol) and **5** in the solvent (5 mL) at –78°C, which was stirred at the temperature for 4 h. Yields refer to the ^{19}F NMR yield using bis(4-fluorophenyl)methanone as the internal standard compound; dr values were determined by ^{19}F NMR; isolated yield was reported in the parathesis.n.d., not determined. CPME, cyclopentyl methyl ether; DBU, 1,8-diazabicyclo[5.4.0]undec-7-ene; DME, dimethyl ether; HMDS, hexamethyldisilazide; MTBE, *tert*-butyl methyl ether; TBS, *tert*-butyl dimethyl silyl; THF, tetrahydrofuran. [a]0°C.

fluoro(chloro)alkenes **6** of only 16% was observed via ^{19}F NMR spectroscopy, and the *Z*/*E* ratio was 95/5 (entry 3). However, sodium hexamethyldisilazide (NaHMDS) proved substantially more effective, delivering the persubstituted fluoro(chloro)alkene in 81% yield while maintaining high stereoselectivity (*Z*/*E* = 95:5, entry 4). Potassium hexamethyldisilazide (KHMDS) and potassium *tert*-butoxide (*t*BuOK) generated the target product (entries 5 and 6) in much lower yields than NaHMDS. It was found that the use of DBU as the base cannot yield the fluoro(chloro)alkene, likely due to insufficient basicity (entry 7). With NaHMDS as the optimal base, solvents were screened, and dimethyl ether (DME) gave the highest yield and stereoselectivity (entries 8–14). Final optimization of the reaction conditions by changing the ratio of **4**:**5**:base to 1.0:2.5:2.5 led to the formation of **6** in 91% NMR yield (88% isolated yield, entry 15). Interestingly, at 0°C, it was found that it did not affect the *Z*/*E* selectivity, although the yield decreased (entry 16).

2.2 | Substrate Scope Study of Stereoselective *Gem*-Fluoro(chloro)-olefination

We subsequently investigated the scope of the reaction between various ketones and sulfoximine **4**. The results are summarized in Figure 3. A variety of structurally diverse aromatic ketones were successfully converted to persubstituted *gem*-fluoro(chloro)alkenes in good yields with high stereoselectivities. The reaction accommodated diverse substituents, such as chloro, bromo, iodo, and benzoxy (products **11**–**14**). Products bearing a tertiary amine (**15**), a boronic ester (**16**), a silyl group (**17**), a phosphorus group (**18**), a trifluoromethylthio group (**19**), a difluoromethoxy group (**20**), carboxylic ester groups (**21**), a cyanide group (**22**), and a sulfonyl group (**23**) were obtained in yields of 70%–89% and *Z*/*E* ratios of 92:8–98:2. The stereochemical outcome remained high regardless of the electronic properties or positioning of substituents on aromatic rings, indicating the robustness of the method (products **21**–**25**). Moreover, products bearing propargyl ether (**26**), homoallyl silyl ether (**27**), or a highly functionalized spiro azetidine (**28**) were obtained in yields of 83%–87% and *Z*/*E* ratios of 95:5–98:2.

Substrates with multiple substituents showed that the reaction was not sensitive to multiple substituents on the aromatic rings (**29**-**32**). Pharmaceutically important heteroaromatic groups [51, 52], such as nitrogen-containing groups (2-pyrrolyl, 3-pyrrolyl, and indolyl), sulfur-containing moieties (benzothienyl and benzothiazolyl), and saturated heterocycles (morpholinyl) were well tolerated, affording products **33**–**38** in yields of 65%–88% with *Z*/*E* ratios of 94:6–98:2.

Furthermore, substrates with various alkyl chains, including an ethyl group, a fluoromethyl group, a hydroxymethyl group, and a trideuterium methyl group, gave products **39** (78% yield, 94:6 *Z*/*E*), **40** (31% yield, 96:4 *Z*/*E*), **41** (47% yield, 92:8 *Z*/*E*), and **42** (65% yield, 97:3 *Z*/*E*) respectively. Ketone bearing various cycloalkyl groups (cyclopropyl, cyclobutyl, and cyclopentyl) and 1-indanone, gave products **43** (54% yield, 97:3 *Z*/*E*), **44** (65% yield, 92:8 *Z*/*E*), **45** (68% yield, 94:6 *Z*/*E*), and **46** (71% yield, 92:8 *Z*/*E*), respectively. The slightly diminished yield for the cyclopropyl derivative may reflect ring strain increased in the transition state. Additionally, the scope could be further extended to enones (**47**, 43% yield, >98:2 *Z*/*E*), and 1-acetyl ferrocene (**48**, 69% yield, >98:2 *Z*/*E*).

For alkyl-alkyl substrates, α-branched dialkyl ketones derived from ibuprofen and naproxen, afforded products **49** and **50** in good yields and high *Z*/*E* ratios (**49**, 71% yield, >98:2 *Z*/*E*; and **50**, 68% yield, 98:2 *Z*/*E*). The method tolerated homoallylic and allylic ethers (**51**, 58% yield, 90:10 *Z*/*E*; and **52**, 65% yield, 91:9 *Z*/*E*), as well as cyclic substrates such as cyclohexanone (**53**, 49% yield,

15213773, 2026, 15, Downloaded from https://onlinelibrary.wiley.com/doi/10.1002/anie.511068 by Shanghai Institute Of Organic Chemistry, Wiley Online Library on [03/11/2026]. See the Terms and Conditions (https://onlinelibrary.wiley.com/terms-and-conditions) on Wiley Online Library for rules of use; OA articles are governed by the applicable Creative Commons License

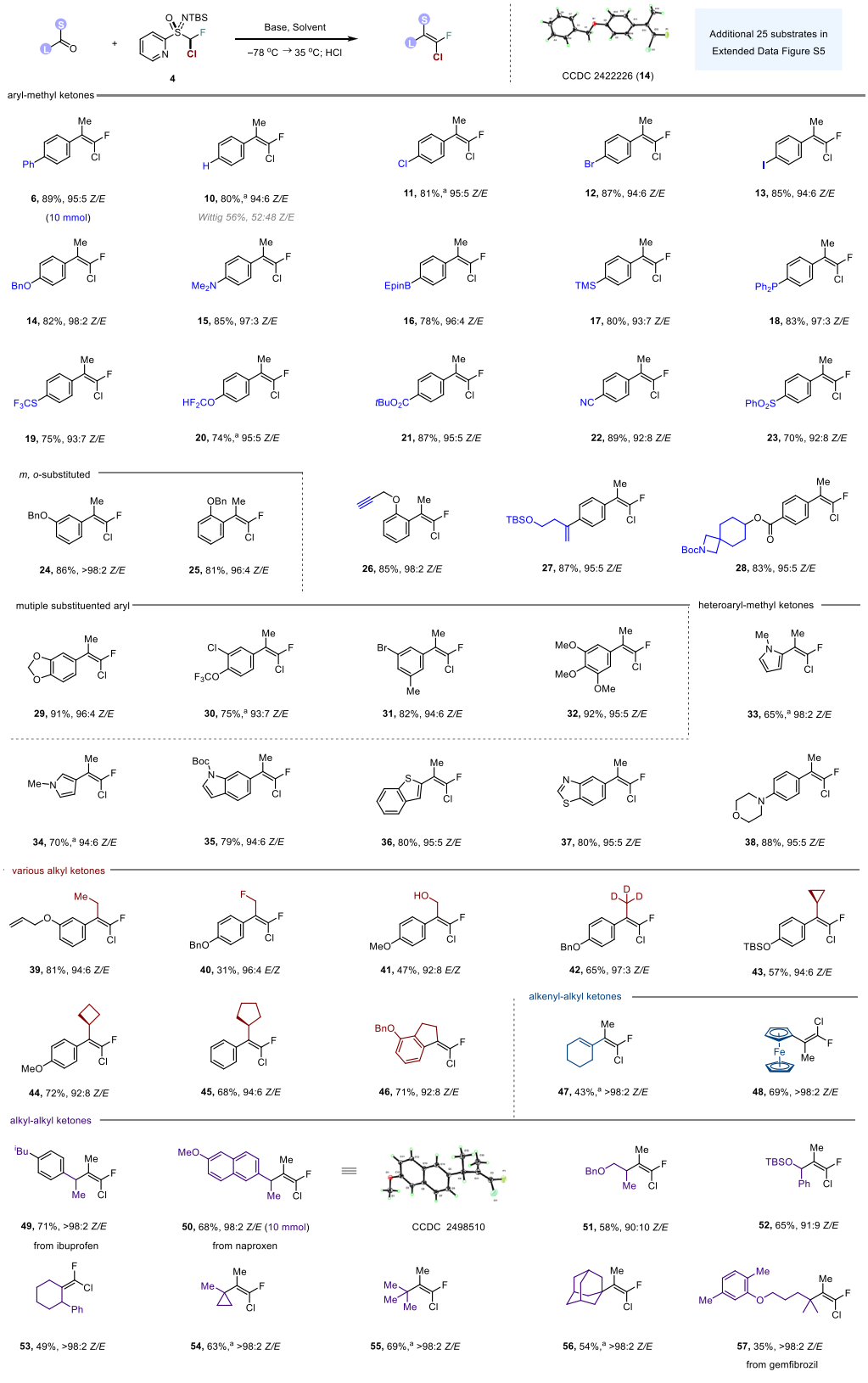


FIGURE 3 | Substrate scope for stereoselective *gem*-fluoro(chloro)-olefination of carbonyl compounds. General reaction conditions: NaHMDS was added slowly to the mixture of **4** (0.2 mmol) and ketones in the solvent (5 mL) at −78°C, which was stirred at the temperature for 4 h. The yields refer to the isolated yield of the desired products. The *Z*/*E* ratios were determined by ^{19}F NMR analysis of the crude product unless otherwise specifically noted.[a] The products are volatile, and the yields and *Z*/*E* ratios were determined by ^{19}F NMR analysis. B(Epin), 1,1,2,2-tetraethylethylene glycol boronate ester; Boc, *tert*-butoxylcarbonyl; Cy, cyclohexyl; TMS, trimethylsilyl.

15213773, 2026, 15, Downloaded from https://onlinelibrary.wiley.com/doi/10.1002/anie.511068 by Shanghai Institute Of Organic Chemistry, Wiley Online Library on [03/11/2026]. See the Terms and Conditions (https://onlinelibrary.wiley.com/terms-and-conditions) on Wiley Online Library for rules of use; OA articles are governed by the applicable Creative Commons License

>98:2 *Z*/*E*). The reaction also tolerated more sterically hindered tertiary alkyl substituents, yielding products **54**–**57** in yields of 35%–69% and *Z*/*E* ratios of >98:2, from a ketone derivative from gemfibrozil.

And an additional 25 examples in Supporting Information further highlighted the generality of this protocol (Figure S5). The configuration of **14** and **50** was established by X-ray analysis [50], whereas those of the other compounds were assigned by analogy.

We scaled up the reaction to a scale of 10 mmol, with products **6** and **50** yielding comparably to standard conditions. Finally, and notably, comparative studies with classical Wittig conditions revealed the superior performance of our protocol [53].

2.3 | Downstream Transformations and Microfluidic Reactor Synthesis

The synthetic utility of the methodology was further demonstrated by the chemoselective transformation of the C—Cl bond in compound **6**, affording diverse derivatives with complete retention of stereochemical configuration (Figure 4a). In particular, we prepared a deuterium-labeled fluoroalkenes (**58**), which holds significant potential for mechanistic and metabolic studies. The chlorine substituent was exchanged by alkyl (**59**), allyl (**60**), allylic alcohol (**61**), alkenyl (**62**), alkynyl (**63**), aryl (**64**), and heteroaryl (**65** and **66**) groups. Furthermore, the prepared alkenyl boronates (**67**) and halogenated derivatives (bromo-**74**; iodo-**75**) were shown to serve as highly effective cross-coupling partners, significantly broadening the scope of this synthetic method. The tetrasubstituted 1,4-conjugated enone (**68**) was obtained in 72% yield with *E*/*Z* ratio of 98:2, and acrylonitrile (**69**) was obtained in 76% yield with 95:5 *E*/*Z* ratio of 98:2. In addition, the chlorine substituent was also exchanged with other heteroatoms, exemplified by the preparation of enol ether (**70**), alkenyl sulfides (**71**), alkenyl selenols (**72**), and alkenyl phosphonate (**73**). Significantly noteworthy are trifluoromethyl- and trifluoromethylthio-substituted **76** and **77**, which were obtained in 85% yield with *E*/*Z* ratio of >98:2 and 87% yield with *Z*/*E* ratio of 98:2, respectively. The post transformations of persubstituted *gem*-fluoro(chloro)alkenes magnificently expanded their accessibility. The presented persubstituted alkenyl fluorides are otherwise difficult to access, which demonstrates the potential of this method to advance the related chemistry.

The microfluidic reactor system was performed, because the modular microfluidic reactor systems was considered to provide a stepping stone for practical-scale production [54–57]. The microfluidic *gem*-fluoro(chloro)olefination of **5** was developed, providing the desired product **6** on a scale of 2.12 g (86% yield, *Z*/*E* 96/4) but with much shorter time and at an elevated temperature of –20°C, which facilitated a low-energy-consumption pathway for large-scale synthesis (Figure 4b).

2.4 | Synthetic Applications

We further demonstrated the *gem*-fluoro(chloro)olefination method was suitable for late-stage functionalization of structurally complex molecules (Figure 5a). The method allowed efficient introduction of geminal fluoro(chloro)alkenyl groups into diverse pharmacologically relevant scaffolds including indomethacin (**78**), sertraline (**79**), ergosterol (**80**), naproxen (**81**), pyrrolidinol (**82**), and fluoxetine (**83**). All transformations proceeded with excellent stereoselectivities (*Z*/*E* 94:6–>98:2), underscoring the robustness of the method. Notably, we could successfully modify even highly functionalized carbohydrate derivatives, converting *β*-L-allopyranose-derived ketones to the *gem*-fluoro(chloro)alkene (**84**, 72% yield, *Z*/*E* 98:2) while preserving the acid-sensitive acetal functionality. The sertraline derivatized ethyl ketone was transformed to the corresponding *gem*-fluoro(chloro)alkene (**85**, 43% yield, *Z*/*E* >98:2), exhibiting the compatibility of styryl and sulfoxide functional groups.

To further demonstrate the synthetic utility of the current method, we applied it to the preparations of a factor Xa inhibitor (**90**) [22] and a retinoid X receptor regulator (**94**) [10–13] (Figure 5b,c). With standard conditions, the reaction between sulfoximine **4** and commercially available 1-(isoquinolin-7-yl)ethan-1-one (**86**) proceeded smoothly to give **87** in 81% yield with a *Z*/*E* ratio of 94:6. The chlorine substituent was exchanged with phenyl carboxylate in 78% yield without any loss of the stereoselectivity. Amino-transesterification resulted into the formation of **89**, a key fluorine-containing product for factor Xa inhibitor.

For the synthesis of the retinoid X receptor regulator, we started the route from commercially available **95**, which gave a ketone **96** after the sequence of Friedel–Crafts acetylation and etherification. *gem*-Fluoro(chloro)olefination of **97** with sulfoximine **4** afforded **98** in 81% yield with a *Z*/*E* ratio of 97:3. Final product **94**, which can activate retinoid X receptor regulator and has potential advantageous therapeutic applications in type 2 diabetes [13], was furnished by cross coupling of the *gem*-fluoro(chloro)alkene **98**. The new route to **94** had a 47% total yield over four steps with an *E*/*Z* ratio of 96:4, superior to the previous route with <1% total yield over 11 steps and an *E*/*Z* ratio of 93:7 [11].

For the synthesis of peptide analogue, the compound **6** proceeds Suzuki coupling under palladium catalyst, giving the allylic amine **99**. It was further transformed to compound **101** by amide coupling with compound **100** (Figure 5d).

2.5 | Mechanistic Studies

To gain insights into the reaction mechanism, we started to perform quenching experiments using D_2O (Figure 6a). Low diastereomeric ratio (74:26 dr) was observed for monodeuterated diastereomers **7** and **7′**, indicating that carbanion was formed in both *R* and *S* configurations at the fluorinated carbon were formed. And the DFT-optimized structures of **Int0-R** and **Int0-S** indicates that the negative charge is localized on the carbon atom, as this carbon adopts a trigonal pyramidal geometry. This stabilization arises from the strong electron-withdrawing effect of the fluorine substituent, which stabilizes the carbanion and prevents the formation of an enolate-type structure. The addition of hexamethylphosphoramide (HMPA), a strongly coordinating solvent, did not affect the *Z*/*E* selectivity even though the yield was slightly decreased (Figure 6b), indicating that the nonchelated transition states of the reaction possibly played a crucial role.

15213773, 2026, 15, Downloaded from https://onlinelibrary.wiley.com/doi/10.1002/anie.511068 by Shanghai Institute Of Organic Chemistry, Wiley Online Library on [03/11/2026]. See the Terms and Conditions (https://onlinelibrary.wiley.com/terms-and-conditions) on Wiley Online Library for rules of use; OA articles are governed by the applicable Creative Commons License

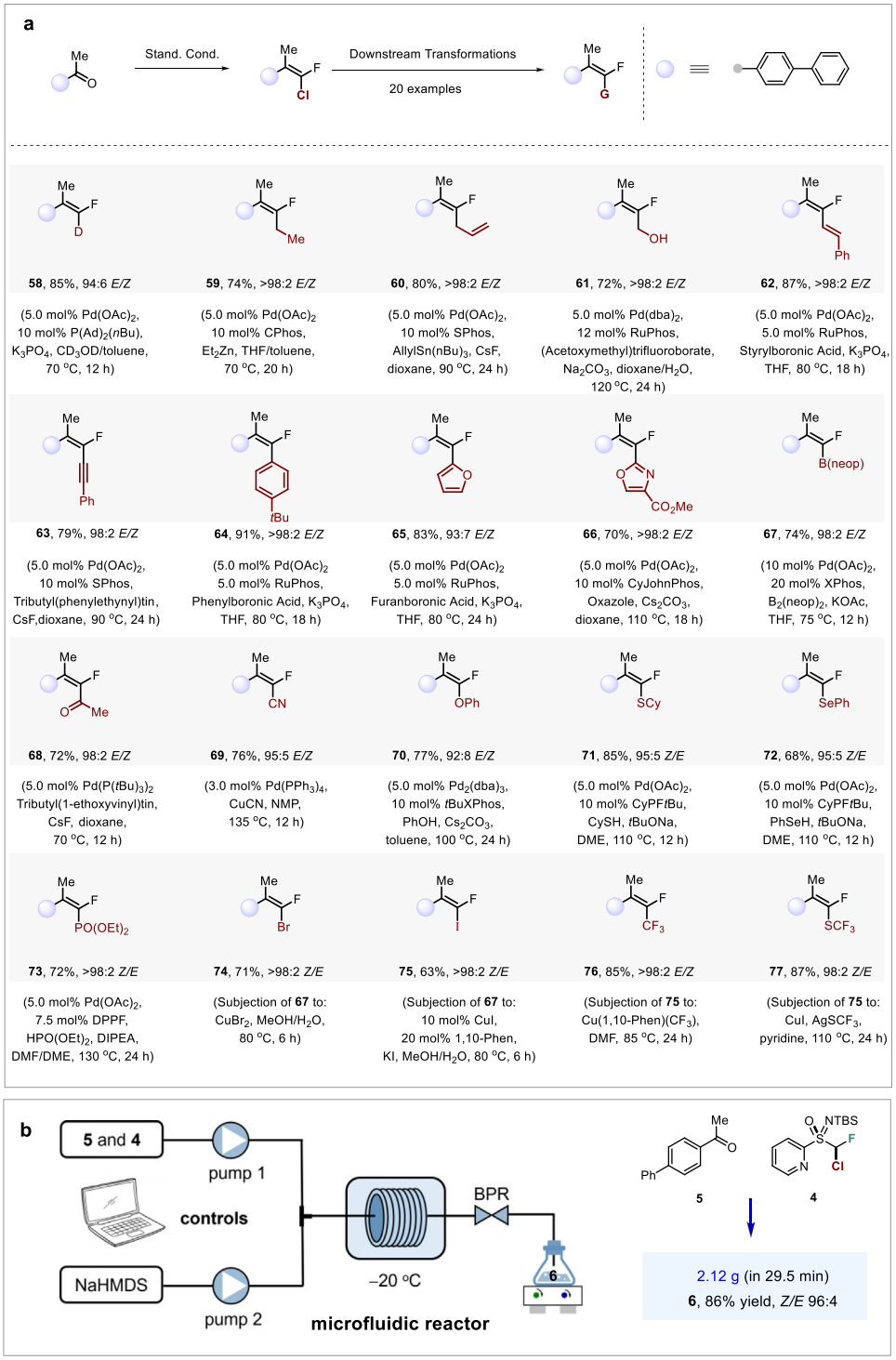


FIGURE 4 | Microfluidic reactor synthesis, and post transformations. (a) Downstream transformations of *gem*-fluoro(chloro)alkenes. (b) Microfluidic reactor synthesis. BPR, back pressure regulator; Cy = cyclohexyl; neop = neopentyl glycol.

Major diastereomer **8** of the nucleophilic addition products was isolated with a dr of >98:2 (see Supporting Information). NaHMDS was added to compound **8** at −78°C and the reaction was quenched at low temperature after 30 min. Fluoro(chloro)methylsulfoximine **4′** was regenerated with a dr of 67:33 (Figure 6c), which indicated the carbonyl adduct reverted to the sulfoximine reagent **4′** and ketone. Furthermore, when compound **8** was subjected to the standard conditions, the (*Z*)-fluoro(chloro)alkene was generated with a *Z*/*E* ratio of 97/3 (Figure 6d). We also conducted the model reaction with diastereomeric mixture **4′**. The persubstituted fluoro(chloro)alkene was obtained in 84% yield with 96:4 Z/E (please see the part 4.4 in Supporting Information for details)

To substantiate our findings, we synthesized the minor diastereomer **9** with a dr of >98:2 via methyl addition. The X-ray crystal

15213773, 2026, 15, Downloaded from https://onlinelibrary.wiley.com/doi/10.1002/anie.511068 by Shanghai Institute Of Organic Chemistry, Wiley Online Library on [03/11/2026]. See the Terms and Conditions (https://onlinelibrary.wiley.com/terms-and-conditions) on Wiley Online Library for rules of use; OA articles are governed by the applicable Creative Commons License

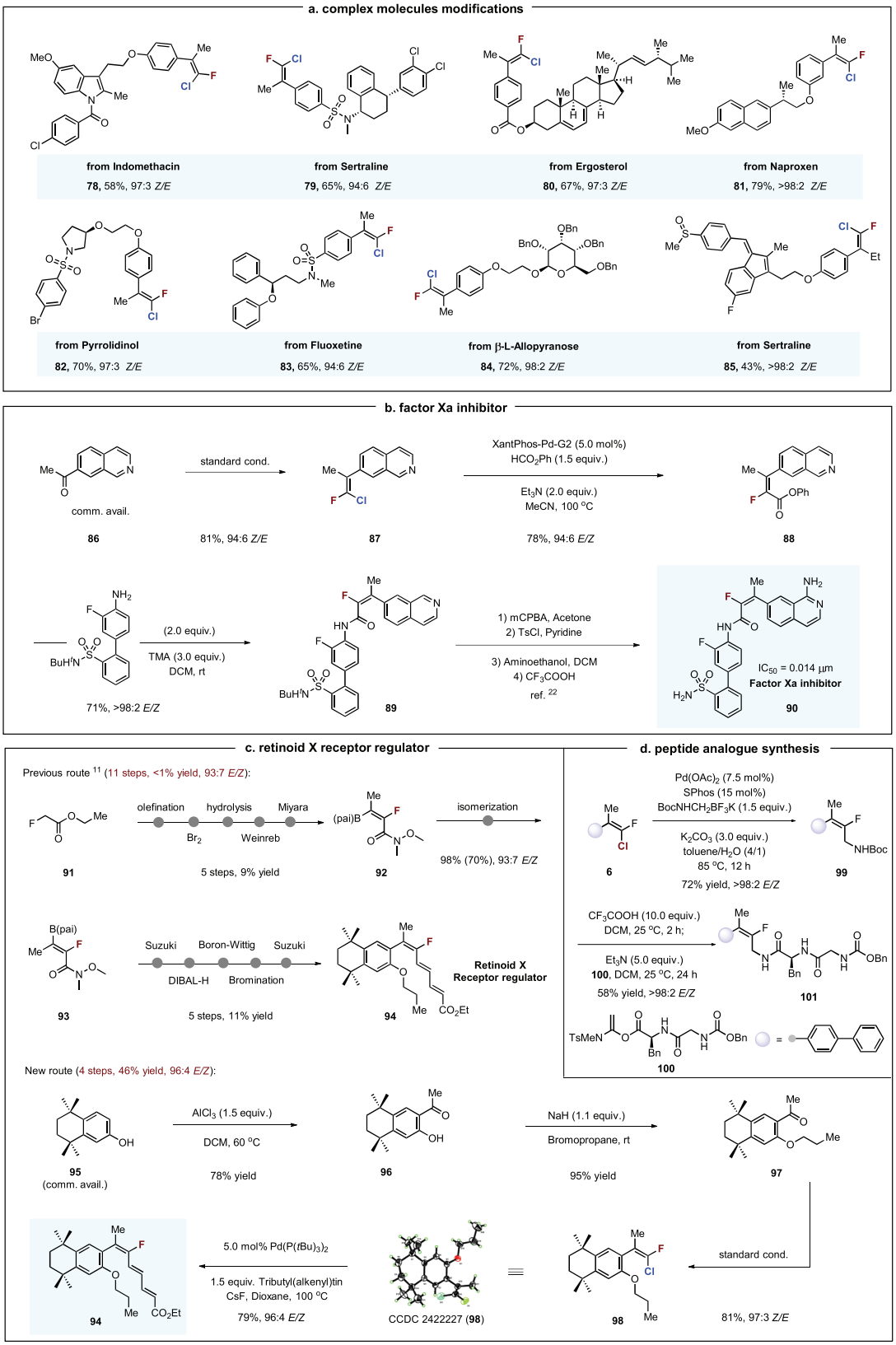


FIGURE 5 | Synthetic applications. (a) Late-stage modifications of complex molecules. (b) Synthetic approach to factor Xa inhibitor. (c) Synthetic approach to retinoid X receptor regulator. B(pai), boronic pinanediol ester; TMA, trimethyl aluminum.

15213773, 2026, 15, Downloaded from https://onlinelibrary.wiley.com/doi/10.1002/anie.511068 by Shanghai Institute Of Organic Chemistry, Wiley Online Library on [03/11/2026]. See the Terms and Conditions (https://onlinelibrary.wiley.com/terms-and-conditions) on Wiley Online Library for rules of use; OA articles are governed by the applicable Creative Commons License

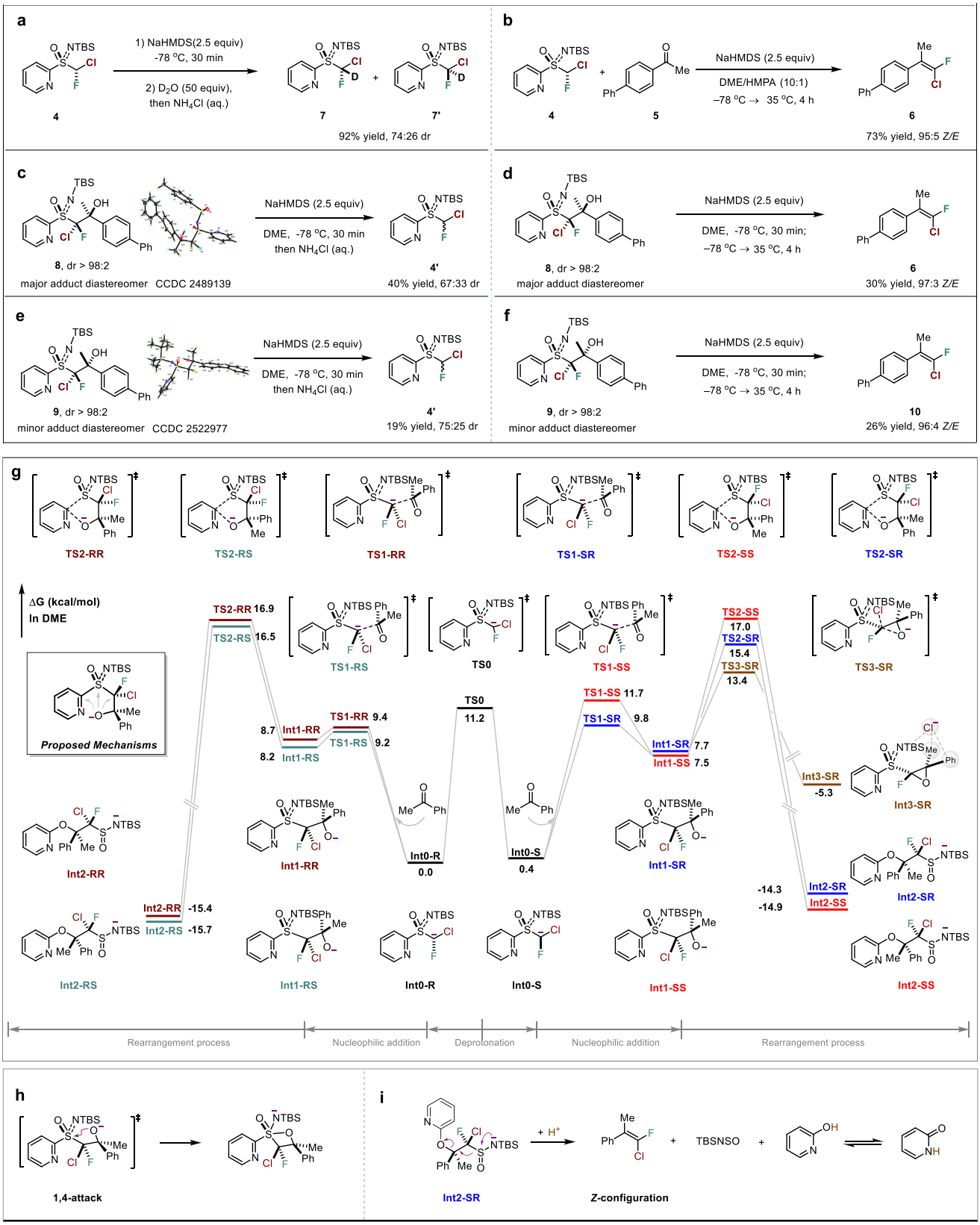


FIGURE 6 | Mechanism studies. (a) The quenching experiment of deuterium water. (b) The reaction was performed when HMPA, a strong coordination solvent, was used. (c) The major carbonyl adduct reacted with NaHMDS. (d) The major carbonyl adduct reacted with standard conditions. (e) The minor carbonyl adduct reacted with NaHMDS. (f) The minor carbonyl adduct reacted with standard conditions. (g) The potential energy surfaces of this reaction (1,5-attack and 1,3-attack). The relative Gibbs free energies are given in kcal/mol. (h) The transition state in which the negatively charged oxygen attacks the sulfur atom (1,4-attack). (i) Upon protonation, *Z*-configured product is generated through antielimination from Int2-SR.

15213773, 2026, 15, Downloaded from https://onlinelibrary.wiley.com/doi/10.1002/anie.511068 by Shanghai Institute Of Organic Chemistry, Wiley Online Library on [03/11/2026]. See the Terms and Conditions (https://onlinelibrary.wiley.com/terms-and-conditions) on Wiley Online Library for rules of use; OA articles are governed by the applicable Creative Commons License

structure analysis of **9** indicated its configuration of hydroxyl-bearing carbon center was opposite to that in major diastereomer **8** (Figure 6e) [50]. Moreover, we found compound **9** reverted to fluoro(chloro)methyl sulfoximine **4′** after the treatment of NaHMDS (Figure 6f). On the other words, it can be hypothesized that if **9** underwent Smiles rearrangement directly, the (*E*)-fluoro(chloro)alkene could be generated. However, the corresponding (*Z*)-alkene served as the major stereoisomer instead of (*E*)-isomer. This strongly suggested that the diastereomer **9** first reverted to the sulfoximine and ketone, and then underwent nucleophilic addition and Smiles rearrangement under the control of more favorable pathway. The lower yield can be attributed to a significantly lower concentration of the ketone available by the reverse reaction.

To elucidate the reaction pathway and the origin of stereoselectivity, we conducted density functional theory (DFT) computational studies and a conformational search (see Supporting Information for more computational details). For computational efficiency, the sulfur stereocenter of the sulfoximine reagent was fixed in the (*R*)-configuration during modeling. This simplification is justified because the reagent we used was racemic; the potential energy surfaces for the diastereomeric pathways originating from the (*S*)-configured sulfur center are mirror images of those from the (*R*)-configuration, and thus would yield enantiomeric outcomes but identical energetic profiles. Frequency analysis was conducted to verify the stationary points to be energy minimum to obtain the thermal energy corrections.

The Gibbs free energies of the most stable conformers for each intermediate and transition state on the potential energy surface (PES) are shown in Figure 6g. Under basic conditions, the substrate underwent deprotonation to form intermediate **Int0-R**, which isomerized to **Int0-S** via a conformational inversion through transition state **TS0** (11.2 kcal/mol). This result was consistent with observations from the deuterium-labeling experiment (see Figure 6a): The DFT-optimized structures of **Int0-R** and **Int0-S** indicates that the negative charge is localized on the carbon atom, as this carbon adopts a trigonal pyramidal geometry. This stabilization arises from the strong electron-withdrawing effect of the fluorine substituent, which stabilizes the carbanion and prevents the formation of an enolate-type structure. **Int0-R** and **Int0-S** could attack the Re and Si faces of the ketone, leading to the formation of four possible low-energy transition states, **TS1-RS**, **TS1-RR**, **TS1-SR**, and **TS1-SS**, each corresponding to a distinct intermediate, Int1. The negatively charged oxygen in **Int1** can undergo intramolecular nucleophilic attack on the pyridyl, the sulfur atom, or the chlorine-bearing carbon center, leading to the formation of five-, four-, and three-membered ring transition states, respectively (see the proposed mechanisms in Figure 6g).

In the 1,5-attack pathway (Figure 6g), the negatively charged oxygen in Int1 lanuched intramolecular nucleophilic attack on the pyridyl via a five-membered ring transition state, **TS2**, to afford **Int2**. According to the Curtin–Hammett principle, although **Int1-SS** (7.5 kcal/mol) was slightly lower in energy than **Int1-SR** (7.7 kcal/mol), the stereoselectivity was governed by **TS2**, which was the rate-determining step (RDS) on the PES. Among the possible transition states, **TS2-SR** had the lowest activation barrier (15.4 kcal/mol), compared with **TS2-RS**, **TS2-RR**, and **TS2-SS**. The higher activation barriers of **TS2-RS** (16.5 kcal/mol) and **TS2-RR** (16.9 kcal/mol) were attributed to steric repulsion between the chlorine atom and the oxygen atom of the S═O group in the five-membered ring transition state. The higher activation barrier of **TS2-SS** (17.0 kcal/mol) was explained by steric hindrance between the Cl atom and the —Ph group in **TS2-SS**. Specifically, in **TS2-SS**, the TBS group restricts the orientation of the phenyl ring, leading to a distance between the chlorine atom and the hydrogen atom on the phenyl ring that is shorter than the sum of their van der Waals radii, thereby resulting in a pronounced Cl–Ph steric repulsion. In contrast, in **TS2-RR**, the orientation of the phenyl ring is not constrained by the TBS group, and therefore no significant steric interaction between the chlorine atom and the phenyl ring is observed. The results indicated that the chlorine atom dictated stereoselectivity through steric effects by enforcing a kinetically controlled rate-determining 1,5-rearrangement. This pathway was uniquely favored over the three others, which was consistent with observations of the stereomeric convergence of two diastereomers **8** and **9** (Figure 6d,f).

In the 1,3-attack pathway (Figure 6g, brown color), the negatively charged oxygen in **Int1** attacked the chlorine-bearing carbon center via a three-membered ring transition state, T**S3**. We calculated the activation barrier of **TS3-SR**, which was associated with **Int1-SR**. Although **TS3-SR** had a relatively low activation barrier of 13.4 kcal/mol, the resulting intermediate, **Int3-SR**, was not sufficiently stable (–5.3 kcal/mol).

According to the principle of microscopic reversibility, **Int3-SR** could undergo a reversible reaction back to **Int1-SR** at room temperature. In contrast, **Int2-SR**, which was formed via **TS2-SR**, was much more stable (–14.3 kcal/mol). Therefore, given sufficient reaction time, the reaction would preferentially proceed through the five-membered-ring transition state **TS2-SR** to afford **Int2-SR**. Nevertheless, the 1,3-attack pathway cannot be excluded as a potentially significant competing pathway. Finally, upon protonation, **Int2-SR** underwent *anti*-elimination to form the (*Z*)-stereoisomer (Figure 6i).

And in the 1,4-attack pathway (Figure 6h), the negatively charged oxygen attacked the sulfur atom forming a four-membered-ring intermediate, which could undergo elimination to afford the alkene product. However, this transition state could not be located using DFT calculations. We performed a relaxed scan along the forming S—O bond and observed a continuous increase in energy as the S—O bond length decreased from 2.67 to 1.96 Å, suggesting that the four-membered ring intermediate is not a stable minimum on the PES (please see Supporting Information for more details). As a result, this pathway was excluded from further consideration.

For a summary of all proposed mechanistic pathways, please refer to the Supporting Information.

3 | Conclusion

In summary, we developed a *gem*-fluoro(chloro)methyl sulfoximine reagent, which enabled a straightforward, stereoselective *gem*-fluoro(chloro)olefination, thereby addressing the long-standing challenge of how to access (Z)-persubstituted *gem*-fluoro(chloro)alkenes. This operationally simple protocol

15213773, 2026, 15, Downloaded from https://onlinelibrary.wiley.com/doi/10.1002/anie.511068 by Shanghai Institute Of Organic Chemistry, Wiley Online Library on [03/11/2026]. See the Terms and Conditions (https://onlinelibrary.wiley.com/terms-and-conditions) on Wiley Online Library for rules of use; OA articles are governed by the applicable Creative Commons License

transformed ubiquitous carbonyl compounds into fluoroalkenes with the retained C—Cl bond as a versatile linchpin, whose downstream diversification provided a wide array of fluorinated architectures by easy cross couplings. The versatility of this platform was underscored by its applications to microfluid synthesis, late-stage modifications, and a streamlined stereoselective synthesis of factor Xa inhibitor and retinoid X receptor regulator. The experimental and computational studies revealed the exceptional efficiency and stereocontrol stemmed from a unique interplay, that the electrophilic pyridyl group suppressed premature C—Cl cleavage while the chlorine atom dictated stereoselectivity, enforcing a kinetically-controlled rate-determining 1,5-rearrangement. More broadly, this work established a general strategy for stereocontrol in challenging olefinations by leveraging kinetic gating through synergistic steric and electronic interplay. The design principles uncovered—employing a heterocyclic stabilizer to suppress undesired pathways and a halogen atom to steer stereoselectivity via spatial constraints—offer a general blueprint for developing next-generation reagent in stereocontrolled synthesis, extending far beyond the realm of fluorine chemistry.

Acknowledgments

We thank Prof. Takatsugu Murata at Tokyo University of Science for insightful discussions and suggestions. This project was supported by the National Natural Science Foundation of China (Grant Number. 22577152 to Qinghe Liu and 22403067 to Tian-Yu Sun), the National Natural Science Fund for Excellent Young Scholars (Overseas to Qinghe Liu), the Foundation of State Key Laboratory of Natural Medicines (SKLNMZZ2024JS15 to Qinghe Liu), the Foundation of NHC Key Laboratory of Nuclear Technology Medical Transformation (MIANYANG CENTRAL HOSPITAL) (2025HYX014 to Qinghe Liu), Natural Science Foundation of Jiangsu Province, China (Grant Number BK20251582 to Jing Zhang), and National Innovation and Entrepreneurship Training Program for Undergraduate (to Qingyuan Zhao). This work was supported by Shenzhen Bay Laboratory High Performance Computing and Informatics Facility.

Conflicts of Interest

Qinghe Liu, Han Yu, and Qingyuan Zhao may benefit from a patent based on the method disclosed in this paper. The other authors declare no competing interests.

Data Availability Statement

The data that support the findings of this study are available on request from the corresponding author. The data are not publicly available due to privacy or ethical restrictions.

References

1. K. Müller, C. Faeh, and F. Diederich, "The Unique Role of Fluorine in the Design of Active Ingredients for Modern Crop Protection," *Science* 317 (2007): 1881–1886.

2. P. Jeschke, "The Unique Role of Fluorine in the Design of Active Ingredients for Modern Crop Protection," *Chembiochem* 5 (2004): 570–589, https://doi.org/10.1002/cbic.200300833.

3. R. Berger, G. Resnati, P. Metrangolo, E. Weber, and J. Hulliger, "Organic Fluorine Compounds: A Great Opportunity for Enhanced Materials Properties," *Chemical Society Reviews* 40 (2011): 3496–3508, https://doi.org/10.1039/c0cs00221f.

4. A. A. Berger, J.-S. Völler, N. Budisa, and B. Koksch, "Deciphering the Fluorine Code—The Many Hats Fluorine Wears in a Protein Environment," *Accounts of Chemical Research* 50 (2017): 2093–2103, https://doi.org/10.1021/acs.accounts.7b00226.

5. N. A. Meanwell, "Fluorine and Fluorinated Motifs in the Design and Application of Bioisosteres for Drug Design," *Journal of Medicinal Chemistry* 61 (2018): 5822–5880, https://doi.org/10.1021/acs.jmedchem.7b01788.

6. Y. Zhou, J. Wang, Z. Gu, et al., "Next Generation of Fluorine-Containing Pharmaceuticals, Compounds Currently in Phase II–III Clinical Trials of Major Pharmaceutical Companies: New Structural Trends and Therapeutic Areas," *Chemical Reviews* 116 (2016): 422–518, https://doi.org/10.1021/acs.chemrev.5b00392.

7. P. H. S. Paioti, S. A. Gonsales, S. Xu, et al., "Catalytic and Stereoselective Transformations With Easily Accessible and Purchasable Allyl and Alkenyl Fluorides," *Angewandte Chemie International Edition* 61 (2022): e202208742, https://doi.org/10.1002/anie.202208742.

8. Q. Liu, C. Ni, and J. Hu, "China's Flourishing Synthetic Organofluorine Chemistry: Innovations in the New Millennium," *National Science Review* 4 (2017): 303–325, https://doi.org/10.1093/nsr/nwx058.

9. F.-L. Qing, X.-Y. Liu, J.-A. Ma, Q. Shen, Q. Song, and P. Tang, "A Fruitful Decade of Organofluorine Chemistry: New Reagents and Reactions," *CCS Chem* 4 (2022): 2518–2549, https://doi.org/10.31635/ccschem.022.202201935.

10. J. A. Wiles, A. S. Phadke, M. Deshpande, et al., "Compounds for the Treatment of Medical Disorders," (2017), US 2017/0066783 A1.

11. T. Deng, S. Shan, Z.-B. Li, et al., "A New Retinoid-Like Compound That Activates Peroxisome Proliferator-Activated Receptors and Lowers Blood Glucose in Diabetic Mice," *Biological & pharmaceutical bulletin* 28 (2005): 1192–1196, https://doi.org/10.1248/bpb.28.1192.

12. T. Taguchi and H. Yanai, in *Fluorine in Medicinal Chemistry and Chemical Biology* (Blackwell publishing Ltd, 2009): 257–290, https://doi.org/10.1002/9781444312096.

13. R. A. Altman, K. K. Sharma, L. G. Rajewski, et al., "Tyr^1-ψ[(Z)CF═CH]-Gly^2 Fluorinated Peptidomimetic Improves Distribution and Metabolism Properties of Leu-Enkephalin," *ACS Chemical Neuroscience* 9 (2018): 1735–1742, https://doi.org/10.1021/acschemneuro.8b00085.

14. R. J. Sciotti, M. Pliushchev, P. E. Wiedeman, et al., "The Synthesis and Biological Evaluation of a Novel Series of Antimicrobials of the Oxazolidinone Class," *Bioorganic & medicinal chemistry letters* 12 (2002): 2121–2123, https://doi.org/10.1016/S0960-894X(02)00352-9.

15. T. Narumi, K. Tomita, E. Inokuchi, et al., "Diastereoselective Synthesis of Highly Functionalized Fluoroalkene Dipeptide Isosteres and Its Application to Fmoc-based Solid-phase Synthesis of a Cyclic Pentapeptide Mimetic," *Tetrahedron* 64 (2008): 4332–4346, https://doi.org/10.1016/j.tet.2008.02.076.

16. S. Kumari, A. V. Carmona, A. K. Tiwari, and P. C. Trippier, "Amide Bond Bioisosteres: Strategies, Synthesis, and Successes," *Journal of Medicinal Chemistry* 63 (2020): 12290–12358, https://doi.org/10.1021/acs.jmedchem.0c00530.

17. S. Osada, S. Sano, M. Ueyama, Y. Chuman, H. Kodama, and K. Sakaguchi, "Fluoroalkene Modification of Mercaptoacetamide-Based Histone Deacetylase Inhibitors," *Bioorganic & Medicinal Chemistry* 18 (2010): 605–611, https://doi.org/10.1016/j.bmc.2009.12.005.

18. L. E. Zimmer, C. Sparr, and R. Gilmour, "Fluorine Conformational Effects in Organocatalysis: An Emerging Strategy for Molecular Design," *Angewandte Chemie International Edition* 50 (2011): 11860–11871, https://doi.org/10.1002/anie.201102027.

19. C. E. Jakobsche, G. Peris, and S. J. Miller, "Functional Analysis of an Aspartate-Based Epoxidation Catalyst With Amide-to-Alkene Peptidomimetic Catalyst Analogues," *Angewandte Chemie International Edition* 47 (2008): 6707–6711, https://doi.org/10.1002/anie.200802223.

20. Y. Song, L. Clizbe, C. Bhakta, et al., "Substituted Acrylamides as Factor Xa Inhibitors: Improving Bioavailability by P1 Modification," *Bioorganic*

15213773, 2026, 15, Downloaded from https://onlinelibrary.wiley.com/doi/10.1002/anie.511068 by Shanghai Institute Of Organic Chemistry, Wiley Online Library on [03/11/2026]. See the Terms and Conditions (https://onlinelibrary.wiley.com/terms-and-conditions) on Wiley Online Library for rules of use; OA articles are governed by the applicable Creative Commons License

& medicinal chemistry letters 12 (2002): 2043–2046, https://doi.org/10.1016/S0960-894X(02)00304-9.

21. M. Drouin, J.-D. Hamel, and J.-F. Paquin, "Synthesis of Monofluoroalkenes: A Leap Forward," *Synthesis* 50 (2018): 881–955.

22. H. Yanai and T. Taguchi, "Synthetic Methods for Fluorinated Olefins," *European Journal of Organic Chemistry* 2011 (2011): 5939–5954, https://doi.org/10.1002/ejoc.201100495.

23. Y. Yamaki, A. Shigenaga, J. Li, Y. Shimohigashi, and A. Otaka, "Synthesis of Amide-Type Fluoroalkene Dipeptide Isosteres by an Intramolecular Redox Reaction," *Journal of Organic Chemistry* 74 (2009): 3278–3285, https://doi.org/10.1021/jo900135t.

24. S. Han, Y. Lee, Y. Jung, and S. H. Cho, "Stereoselective Access to Tetra- and Tri-Substituted Fluoro- and Chloro-Borylalkenes via Boron-Wittig Reaction," *Angewandte Chemie International Edition* 61 (2022): e202210532, https://doi.org/10.1002/anie.202210532.

25. Q. Liu, Y. Mu, T. Koengeter, R. R. Schrock, and A. H. Hoveyda, "Stereodefined alkenes With a Fluoro-chloro Terminus as a Uniquely Enabling Compound Class," *Nature Chemistry* 14 (2022): 463–473, https://doi.org/10.1038/s41557-022-00893-5.

26. Y. U. Sakaguchi, M. Ohashi, T. Niwa, S. Ogoshi, and T. Hosoya, "Copper-Catalyzed Regioselective Monodefluoroborylation of Polyfluoroalkenes En Route to Diverse Fluoroalkenes," *Journal of the American Chemical Society* 139 (2017): 12855–12862, https://doi.org/10.1021/jacs.7b08343.

27. S. Morand, P. Jubault, J.-P. Bouillon, and S. Couve-Bonnaire, "Gem -Heteroatom-Substituted Fluoroalkenes as Mimics of Amide Derivatives or Phosphates: A Comprehensive Review," *Chemistry—A European Journal* 27 (2021): 17273–17292, https://doi.org/10.1002/chem.202102548.

28. M. J. Koh, T. T. Nguyen, H. Zhang, R. R. Schrock, and A. H. Hoveyda, "Direct Synthesis of Z-alkenyl Halides Through Catalytic Cross-metathesis," *Nature* 531 (2016): 459–465, https://doi.org/10.1038/nature17396.

29. T. Yamamoto and T. Yamakawa, "Pd-Catalyzed Arylation of Chlorotrifluoroethylene Using Arylboronic Acids," *Organic Letters* 14 (2012): 3454–3457, https://doi.org/10.1021/ol3014107.

30. C. Xu, S. Chen, L. Lu, and Q. Shen, "Preparation of Trifluorostyrenes Via Palladium-Catalyzed Coupling of Arylboronic Acids With Chloro- and Bromotrifluoroethylene," *Journal of Organic Chemistry* 77 (2012): 10314–10320, https://doi.org/10.1021/jo301998g.

31. P. J. Verardi, E. A. Ryutov, P. Mukherjee, et al., "Stereo-reversed E2 Unlocks *Z*-selective C–H Functionalization," *Science* 389 (2025): 1239–1245, https://doi.org/10.1126/science.adv7630.

32. D. Andrei and S. F. Wnuk, "Synthesis of the Multisubstituted Halogenated Olefins Via Cross-Coupling of Dihaloalkenes With Alkylzinc Bromides," *Journal of Organic Chemistry* 71 (2006): 405–408, https://doi.org/10.1021/jo051980e.

33. V. G. Nenajdenko, A. V. Shastin, V. N. Korotchenko, G. N. Varseev, and E. S. Balenkova, "A Novel Approach to 2-Chloro-2-Fluorostyrenes," *European Journal of Organic Chemistry* 2003 (2003): 302–308, https://doi.org/10.1002/ejoc.200390033.

34. M. Wienhold, B. Kweon, C. McLaughlin, et al., "Geometric Isomerisation of Bifunctional Alkenyl Fluoride Linchpins: Stereodivergence in Amide and Polyene Bioisostere Synthesis," *Angewandte Chemie International Edition* 62 (2023): e202304150, https://doi.org/10.1002/anie.202304150.

35. W. Zhang, W. Huang, and J. Hu, "Highly Stereoselective Synthesis of Monofluoroalkenes From α-Fluorosulfoximines and Nitrones," *Angewandte Chemie International Edition* 48 (2009): 9858–9861, https://doi.org/10.1002/anie.200905077.

36. Y. Nomura, E. Tokunaga, and N. Shibata, "Inherent Oxygen Preference in Enolate Monofluoromethylation and a Synthetic Entry to Monofluoromethyl Ethers," *Angewandte Chemie International Edition* 50 (2011): 1885–1889, https://doi.org/10.1002/anie.201006218.

37. X. Shen and J. Hu, "Fluorinated Sulfoximines: Preparation, Reactions and Applications," *European Journal of Organic Chemistry* 2014 (2014): 4437–4451, https://doi.org/10.1002/ejoc.201402086.

38. V. Bizet, R. Kowalczyk, and C. Bolm, "Fluorinated Sulfoximines: Syntheses, Properties and Applications," *Chemical Society Reviews* 43 (2014): 2426–2438, https://doi.org/10.1039/c3cs60427f.

39. Q. Liu, C. Ni, Q. Wang, D. Meng, and J. Hu, "Difluoromethyl 2-Pyridyl Sulfoximine: A Stereoselective Nucleophilic Reagent for Difluoro(aminosulfinyl)Methylation and Difluoro(aminosulfonyl) Methylation," *CCS Chem* 4 (2022): 3648–3659, https://doi.org/10.31635/ccschem.022.202101634.

40. M. Daniel, G. Dagousset, P. Diter, et al., "Fluorinated Sulfilimino Iminiums: Efficient and Versatile Sources of Perfluoroalkyl Radicals Under Photoredox Catalysis," *Angewandte Chemie International Edition* 56 (2017): 3997–4001, https://doi.org/10.1002/anie.201700290.

41. Y. Macé and E. Magnier, "The New Age of Electrophilic Perfluoroalkylation Reactions," *European Journal of Organic Chemistry* 2012 (2012): 2479–2494.

42. Q. Liu, X. Shen, C. Ni, and J. Hu, "Stereoselective Carbonyl Olefination With Fluorosulfoximines: Facile Access to *Z* or *E* Terminal Monofluoroalkenes," *Angewandte Chemie International Edition* 56 (2017): 619–623, https://doi.org/10.1002/anie.201610127.

43. X. Shen, Q. Liu, W. Zhang, and J. Hu, "Stereoselective Synthesis of (Sulfonimidoyl)Cyclopropanes With (*R*)-PhSO(NTs)CH_2Cl and α,β-Unsaturated Weinreb Amides: Tuning the of Selectivity Between C–Cl and C–S Bond Cleavage," *European Journal of Organic Chemistry* 2016 (2016): 906–909, https://doi.org/10.1002/ejoc.201501611.

44. A. K. Saikia and S. Tsuboi, "Chemistry of Trichlorofluoromethane: Synthesis of Chlorofluoromethyl Phenyl Sulfone and Fluoromethyl Phenyl Sulfone and Some of Their Reactions," *Journal of Organic Chemistry* 66 (2001): 643–647, https://doi.org/10.1021/jo000825r.

45. B. Zajc and R. Kumar, "Synthesis of Fluoroolefins via Julia-Kocienski Olefination," *Synthesis* 2010 (2010): 1822–1836, https://doi.org/10.1055/s-0029-1218789.

46. A. B. Flynn and W. W. Ogilvie, "Stereocontrolled Synthesis of Tetrasubstituted Olefins," *Chemical Reviews* 107 (2007): 4698–4745, https://doi.org/10.1021/cr050051k.

47. B. Gao, Y. Zhao, M. Hu, C. Ni, and J. Hu, "*gem*-Difluoroolefination of Diaryl Ketones and Enolizable Aldehydes With Difluoromethyl 2-Pyridyl Sulfone: New Insights Into the Julia–Kocienski Reaction," *Chemistry—A European Journal* 20 (2014): 7803–7810, https://doi.org/10.1002/chem.201402183.

48. H. Albright, A. J. Davis, J. L. Gomez-Lopez, et al., "Carbonyl–Olefin Metathesis," *Chemical Reviews* 121 (2021): 9359–9406, https://doi.org/10.1021/acs.chemrev.0c01096.

49. H. Tang, M. Zhang, Y. Zhang, P. Luo, D. Ravelli, and J. Wu, "Direct Synthesis of Thioesters From Feedstock Chemicals and Elemental Sulfur," *Journal of the American Chemical Society* 145 (2023): 5846–5854, https://doi.org/10.1021/jacs.2c13157.

50. CCDC2376317(**4**), CCDC 2376318 (**8**), CCDC 2522977 (**9**), CCDC 2422226 (**14**), CCDC 2498510 (**50**), and CCDC 2422227 (**98**) contain the supplementary crystallographic data for this paper. The data can be obtained free of charge from The Cambridge Crystallographic Data Centre via, www.ccdc.cam.ac.uk/data_request/cif.

51. V. Dhayalan, V. S. Dodke, M. P. Kumar, et al., "Recent Synthetic Strategies for the Functionalization of Fused Bicyclic Heteroaromatics Using Organo-Li, -Mg and -Zn Reagents," *Chemical Society Reviews* 53 (2024): 11045–11099, https://doi.org/10.1039/D4CS00369A.

52. L. D. Pennington and D. T. Moustakas, "The Necessary Nitrogen Atom: A Versatile High-Impact Design Element for Multiparameter Optimization," *Journal of Medicinal Chemistry* 60 (2017): 3552–3579, https://doi.org/10.1021/acs.jmedchem.6b01807.

15213773, 2026, 15, Downloaded from https://onlinelibrary.wiley.com/doi/10.1002/anie.511066 by Shanghai Institute Of Organic Chemistry, Wiley Online Library on [03/11/2026]. See the Terms and Conditions (https://onlinelibrary.wiley.com/terms-and-conditions) on Wiley Online Library for rules of use; OA articles are governed by the applicable Creative Commons License

53. D. J. Burton and H. C. Krutzsch, "The Preparation and Reactions of a Mixed Halogen Ylid," *Tetrahedron Letters* 9 (1968): 71–76, https://doi.org/10.1016/S0040-4039(01)98729-5.

54. L. Capaldo, Z. Wen, and T. Noël, "A Field Guide to Flow Chemistry for Synthetic Organic Chemists," *Chemical Science* 14 (2023): 4230–4247, https://doi.org/10.1039/D3SC00992K.

55. A. Tanimu, S. Jaenicke, and K. Alhooshani, "Heterogeneous Catalysis in Continuous Flow Microreactors: A Review of Methods and Applications," *Chemical Engineering Journal* 327 (2017): 792–821, https://doi.org/10.1016/j.cej.2017.06.161.

56. R. Porta, M. Benaglia, and A. Puglisi, "Flow Chemistry: Recent Developments in the Synthesis of Pharmaceutical Products," *Organic Process Research & Development* 20 (2016): 2–25, https://doi.org/10.1021/acs.oprd.5b00325.

57. L. Rogers and K. F. Jensen, "Continuous Manufacturing—the Green Chemistry Promise?," *Green Chemistry* 21 (2019): 3481–3498, https://doi.org/10.1039/C9GC00773C.

Supporting Information

Additional supporting information can be found online in the Supporting Information section.

Supporting File 1: anie71583-sup-0001-SuppMat.pdf.

15213773, 2026, 15, Downloaded from https://onlinelibrary.wiley.com/doi/10.1002/anie.511068 by Shanghai Institute Of Organic Chemistry, Wiley Online Library on [03/11/2026]. See the Terms and Conditions (https://onlinelibrary.wiley.com/terms-and-conditions) on Wiley Online Library for rules of use; OA articles are governed by the applicable Creative Commons License